- Technical Paper -

EFFECT OF SILICA POWDER ADDITION ON THE EARLY-AGE HYDRATION OF LOW-HEAT PORTLAND CEMENT PASTE

Haoran XIA[*1], Luge CHENG[*2], Zhenli YANG[*1], and Ippei MARUYAMA [*3,4]

ABSTRACT

In this study, X-ray diffraction analysis and proton nuclear magnetic resonance relaxometry are employed to investigate the hydration process of low heat Portland (L5) cement incorporating silica powder (SP) at an early age. The L5-SP paste had a water-to-binder ratio(w/b) of 0.42. The replacement of SP for L5 cement was 0, 18.75, 26, and 41% (by weight of the binder). From the experimental results, SP accelerated the hydration of the cement paste. SP also changed the pore structure of the paste and the composition of the hydration products.

Keywords: Low heat Portland cement, hydration degree, pore structure, C-S-H

1. INTRODUCTION

Low-heat Portland (graded as L5) cement is specifically designed to reduce the heat of hydration and is usually used in mass concrete projects to reduce the risk of temperature-rise cracking [1-2]. L5 cement is considered an environmentally friendly alternative to ordinary Portland cement (OPC) due to its advantages, such as lower energy consumption and CO_2 emissions [3-4].

L5 cement has a lower content of alite (C_3S) and a higher content of belite (C_2S). Compared with OPC, its reaction speed is slow, and the heat of hydration is small [5]. L5 cement is weak due to its early strength, and researchers are exploring ways to overcome the low reactivity of C_2S and improve the early strength of L5 cement [6-7]. Calcium-Silicate-Hydrate (C-S-H) is the main hydration product of Portland cement. The properties of C-S-H largely determine the performance of cement-based materials [8]. To understand the properties of L5 cement, it is very important to clarify the direct relationship between the amount of hydration products, such as C-S-H and $Ca(OH)_2$ [1].

It has been shown that adding silica powder (SP) and fly ash to OPC and adjusting the mixing ratio can achieve a compromise between hardening rate and fluidity [9]. Therefore, understanding the effect of SP, fly ash, metakaolin, etc. on the hydration process of L5 cement and its hydration products is a noteworthy study.

In this study, SP was used to replace some of the L5 cement. C-S-H gels with different calcium-silica (Ca/Si) ratios will be formed. To study the effect of SP incorporation to form C-S-H with different Ca/Si ratios on early-age hydration. The cement samples of early age (1, 3 and 7 days) were measured by X-ray diffraction (XRD) and proton nuclear magnetic resonance relaxometry (^{1}H-NMR relaxometry). XRD was used to analyze the changes in phase content during hydration. The water content and water distribution in the cement paste were analyzed by ^{1}H-NMR.

2. EXPERIMENT PROGRAMS

2.1 Raw materials

In this study, L5 cement provided by the Mitsubishi Materials Corporation was used. The chemical composition of the L5 cement as is shown in Table 1. The mineral composition of cement is presented in Table 2. The mineral composition was determined by Powder X-ray diffraction (XRD) and Rietveld analysis.

Silicon dioxide amorphous (Silica powder) produced by Kanto Chemical Co., Ltd. was used. The relative density of SP is 2.2.

2.2 Specimen preparation

The water-to-binder ratio (w/b) is 0.42. To obtain four target Ca/Si ratios, the replacement ratios of SP were 0%, 18.75%, 26%, and 41%, respectively. The mixing ratios are shown in Table 3.

The L5 cement samples were mixed with deionized water using a planetary centrifugal mixer at 1000 rpm. Mixing was divided into two steps. The first rotation was continued for 90 s to obtain a cement paste with a w/b of 0.3. Then, the remaining water was added, and the paste was mixed for another 90 s. Finally, the cement paste with the target w/b was obtained. To reduce

*1 Dept. of Architecture, University of Tokyo, M.E., JCI student Member
*2 Dept. of Architecture, University of Tokyo, Dr.E., JCI Member
*3 Prof., Dept. of Architecture, University of Tokyo, Dr.E., JCI Member
*4 Visiting Prof., Dept. of Environmental Engineering and Architecture, Nagoya University, JCI Member

the water secretion, remixing was conducted.

Table 1 Chemical composition of the L5cement.

Binder		L5 cement
Density (g/cm^3)		3.22
LOI (%)		1.30
Chemical composition* (%)	SiO_2	25.09
	Al_2O_3	3.21
	Fe_2O_3	3.30
	CaO	62.21
	MgO	0.82
	SO_3	2.83
	Na_2O	0.26
	K_2O	0.30
	Cl^-	0.003
	Total	98.023

Table2 Mineral composition of the Low heat cement

Cement		L5 cement
Mineral composition* (mass %)	C_3S	25.6±0.2
	C_2S	54.0±0.4
	C_4AF	10.2±0.1
	C_3A	3.1±0.1
	CsH_2	2.4±0.1
	$CsH_{0.5}$	3.4±0.2
	M	0.4±0.1
	Cc	0.9±0.2
	Total	100.0±0.1

*: minerals of cement were expressed in cement chemistry notation: C: CaO, S: SiO_2, A: Al_2O_3, F: Fe_2O_3, M:MgO, H: H_2O, s: SO_3, c: CO_2.

Table 3 The mix proportion of samples.

Samples	L5 cement (%)	Silica powder (%)	Target Ca/Si ratio	w/b
L5-SP0	100	0	2.3	0.42
L5-SP18.75	81.25	18.75	1.4	0.42
L5-SP26	74	26	1.1	0.42
L5-SP41	59	41	0.7	0.42

After the mixing at target w/b, the hardening paste will be moved to the thermostatic room at 20±1°C and remixed every 30 min using a spatula until the cement paste exhibits a creamy consistency (around 6 hours) [10,11]. Immediately, the paste was cast into rectangle molds with a length of 40 mm, a width of 20 mm, and a thickness of 1 mm. The molds were sealed, wrapped with plastic foils and placed in a thermostatic room at 20±1 °C. After one day, the specimens were demolded and placed in a thermostatic curing room for sealed curing up to 182 days.

2.3 XRD/ Rietveld analysis

After the samples were stopped for hydration, The L5 cement paste was ground to a powder with a particle size below 75 microns using a ball mill. Then, the powder samples to be tested were made using the "backloading" method. XRD analyzed the powder samples using the internal standard method. Powder X-ray diffraction measurements were performed using the Aeris device from Malvern PANalytical. The measurement conditions were: CuKα radiation, tube voltage 40 kV, current 15 mA, Soller slit: 0.04 rad, divergence slit: 1/4°, 2θ=5-70°. The measurements for each sample were conducted three times to ensure the accuracy and repeatability of the results. And the software TOPAS ver6.0 was used for analysis.

C_3S (Alite), C_2S(Belite), C_3A (Aluminate phase) C_4AF (Ferrite phase), $CaSO_4$-$2H_2O$(Gypsum), $CaCO_3$(calcite), $CaSO_4$-$0.5H_2O$ (bassanite), AFm (hemicarboaluminate, Monocarbonate), C_3AH_6 (Hydrogarnet), Aft (Ettringite), MgO (Periclase), AFm (Monosulphate), CH(Portlandite) were chosen to be quantified. The internal standard method can quantify the amorphous content (use the standard α-Al_2O_3) [12].

2.4 ^{1}H-NMR Relaxometry

^{1}H-NMR relaxometry measurements were conducted using MQC+ (Oxford Instrument) equipped with a digital filter and a φ10 mm probe. The device was connected to a water bath, and the temperature was maintained at 20 °C throughout the experiments[13]. The magnet provided a resonant frequency of 24.2 MHz. The π/2 pulse length was calibrated for each specimen for every measurement, from 2.2 to 2.4 μs. The relaxation delay was 0.5 s.

Chemically bound water (CBW) was quantified following the method described in a previous study by Muller et al. [14]. A solid echo decay signals were acquired for τ from 5 to 25 μs in 1 μs intervals and the signals were decomposed into Gaussian (solid) and exponential (liquid) components. In order to overcome the limitation caused by the instrument dead time, infinitesimal echo time and the ratios of solid water (Gaussian) and mobile water (exponential) at τ = 0 were obtained by extrapolation.

A Carr-Purcell-Meiboom-Gill (CPMG) pulse sequence experiment was employed for all measurements to quantitatively determine the distribution of ^{1}H T_2relaxation times. The data were analyzed using the Butler-Reeds-Dawson (BRD) method, an inverse Laplace transform (ILT) algorithm [15]. The ILT analysis optimized the smoothing parameter α for each dataset, resulting in a continuous T_2 distribution. Signal intensities were integrated, and their ratios were calculated. A multiexponential fitting (N=4) was applied for datasets with four distinct peaks, ensuring consistency with ILT results. The T_2 distribution was used to evaluate water content in hardened cement paste, identifying interlayer water, gel pore water, interhydrate water, and capillary water, in order of increasing relaxation time [16].

3. RESULTS

3.1 Degree of hydration of L5 cement

Fig.1 shows the phase composition of different cements at different ages. The Partial Or No Known Crystal Structure (PONKCS) method was used to analyze water, amorphous C-S-H generated in the process, and unreacted silica powder[17-18]. Fig. 2 shows the results of the hydration degree of cement mineral from XRD/Rietveld.

The hydration level shows that the incorporation of SP increased the reaction rate of the cement. The hydration rate of cement paste was most significantly improved when the substitution rate of SP was 26%, and the average hydration rate was increased by 78.1%, 25.5%, and 18.3% at 1, 3, and 7 days, respectively.

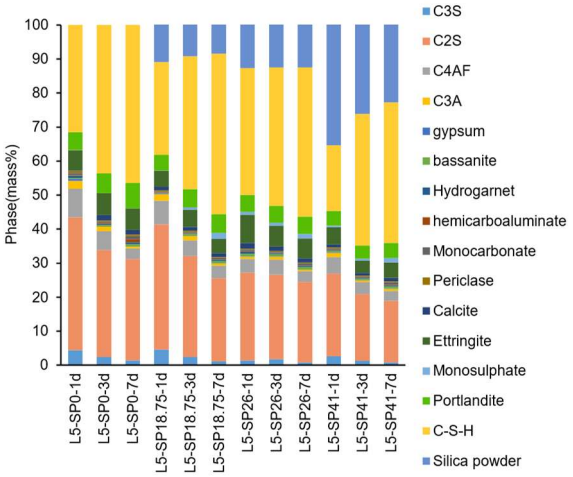

Fig. 1. Phase composition

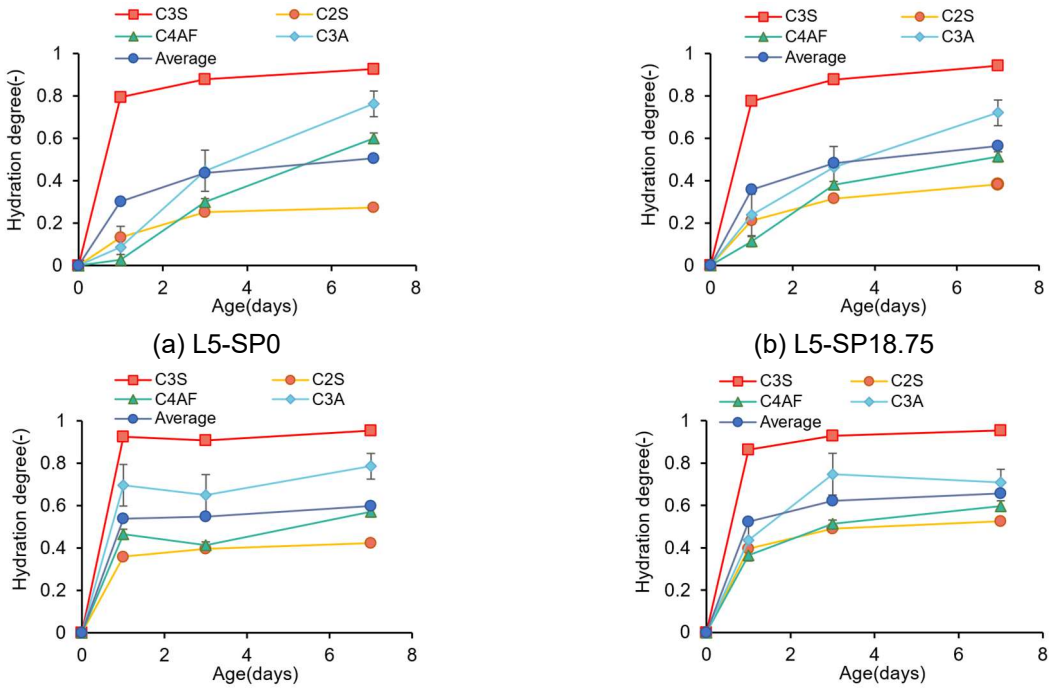

(a) L5-SP0 (b) L5-SP18.75

(c) L5-SP26 (d) L5-SP41

Fig.2. Degree of hydration of each cement minerals and their average.

Fig. 3 shows a comparison of CBW measured by 1H-NMR Relaxometry and the CBW calculated from the phase composition to verify the validity of this development. It can be seen that although the CBW water calculated by the two methods has a similar trend, the content is different. This is mainly because the solid echo signal generated by the solid echo measurement mainly comes from the protons in the crystal (portlandite and ettringite)[14]. Calculating this part of the signal can quantify the CBW water generated during the hydration process of the cement. However, during the hydration process, C-S-H will also contain a large amount of the CBW water. This part of the CBW water in the C-S-H cannot be fully detected in the solid echo signal, resulting in a significant difference between its value and the XRD CBW water calculation result.

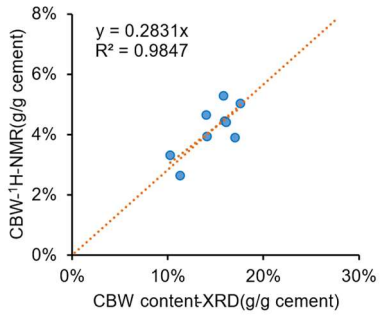

Fig.3. Comparison of CBW obtained by ^{1}H-NMR and calculation results by XRD/Rietveld analysis

3.2 Evolution of T_2 relaxation components

The T_2 distribution calculated from the ILT of the CPMG echo signal decay was normalized [16]. Fig. 4 shows the change in T_2 time during hydration at 1, 3, and 7 days. It can be seen that the T_2 distribution moves from long to short time (towards the left side of the horizontal

axis) as the age increases.

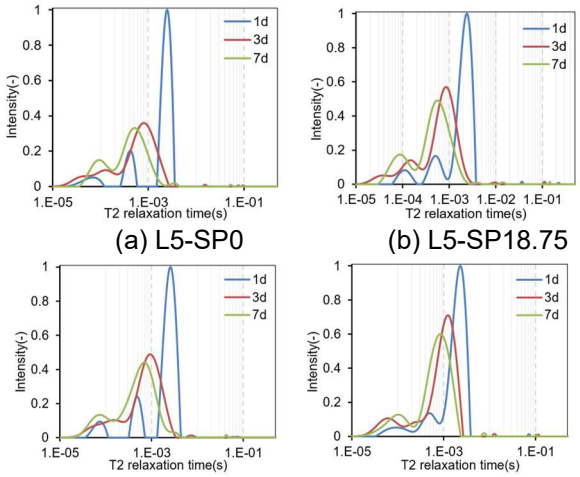

Fig.4. Evolution of the NMR signal of different L5 cement pastes during hydration

As can be seen in Fig. 5, the content of gel water and interlayer water gradually increased with increasing age, and the content of interhydrate water gradually decreased. In terms of the total amount of free water, the mobile water content of the samples showed a decreasing and then increasing trend at 1, 3 and 7 days. It can be found that the presence of SP suppressed the loss of mobile water and the mobile water content of the samples reached the maximum value at 26% SP substitution rate, which was 0.36, 0.34 and 0.33, respectively.

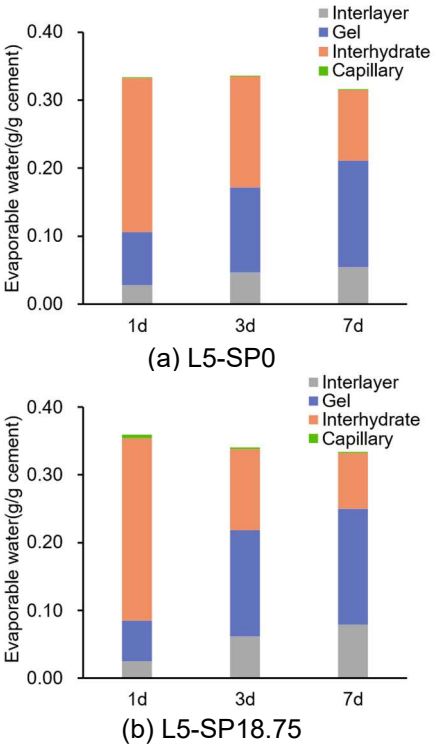

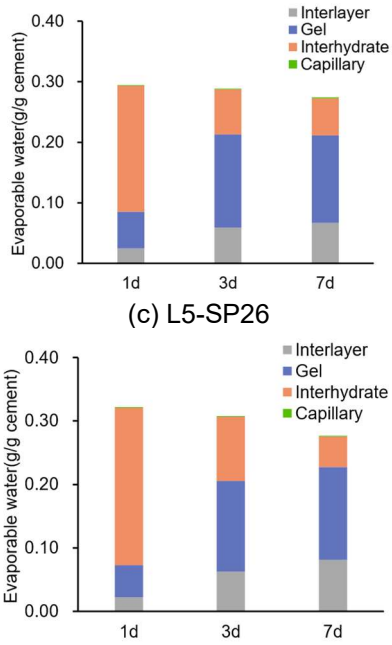

Fig.5. The evolution of water components of L5 cement pastes

3.3 Water content and distribution

By combining solid echo and CPMG pulse sequences, all the water in cement paste can be quantified [19-20]. Based on the pore size, some scholars have classified movable water other than CBW into four categories, interlayer, gel, interhydrate and capillary water[21-22].

Fig. 6 shows the CBW content of L5 cement paste measured by solid echo and CPMG decay. The CBW gradually showed an increasing trend and the evaporable water showed a decreasing trend, but the decreasing trend of evaporable water was mitigated with the addition of SP.

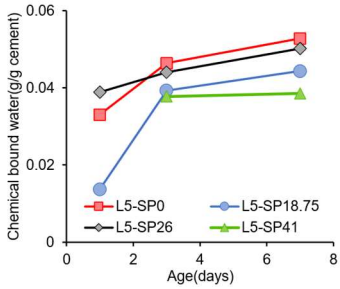

Fig.6. Chemical bound water of L5 cement pastes

4. DISSCUSION

The results of the XRD show that the hydration rate of L5 cement paste was clearly influenced by the incorporation of SP, which agrees with the study of Liao et al.[23]. This can also be verified again by the change in water in the paste. The ratio of CBW to mobile water is gradually increasing. At the same time, the earlier the age, the more obvious the improvement[24]. This is can be attributed to the fact that the pores between the cement particles are filled with SP and the compactness of the system is increased[25-27]. This filling effect can

accelerate cement hydration, especially for the early reaction catalytic effect[23,28-30]. In addition, the surface adsorption of SP promoted the dissolution of cement particles and enhanced the early hydration reaction rate. However, significant hydration rate enhancement was not found when the substitution rate of SP was further increased.

From Fig. 2, it can be seen that the acceleration of SP for the hydration rate of L5 cement originates from the increase in the reaction rate of C_2S, C_3A and C_4AF, which can be inferred to the higher content of C_2S in L5 cement, and the incorporation of SP increases the exposure with C_2S and accelerates its dissolution. Fig. 7 illustrates the increase in the reaction rate of various minerals of the L5 cement by the addition of SP. It can be clearly found that the largest contribution to the hydration degree increase is made at the age of 1 day with a substitution rate of 26%.

The changes in the ratio of CBW to mobile water and the distribution of mobile water also reflected the hydration process of the L5 cement. The decrease in the volume of large pores and the increase in the proportion of the volume of small pores (gel pores) could be attributed to the SP promoted generation of C-S-H further improving the paste compactness[16].

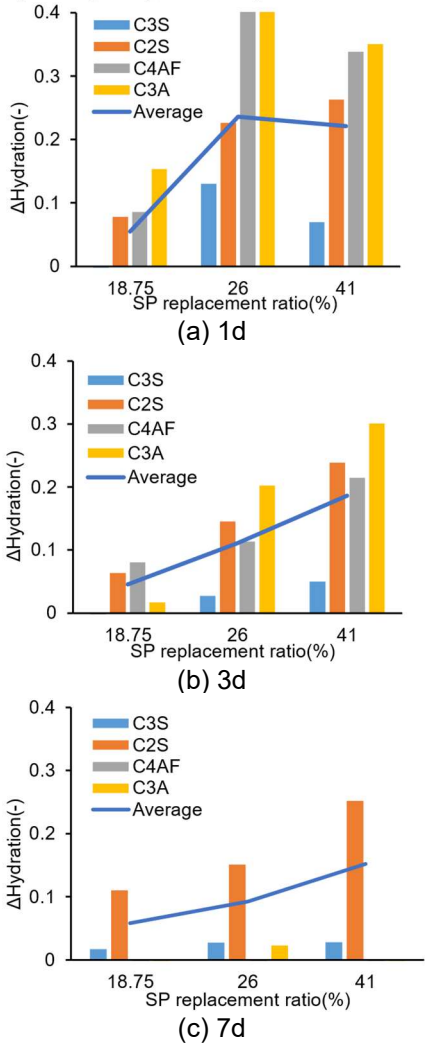

Fig.7. Increase in mineral hydration of L5 cement by SP.

5. CONCLUSIONS

This study investigated the hydration of low-heat cement paste with different replacement ratios of silica powder of 0, 18.75%, 26%, and 41%. Based on X-ray powder diffraction, Rietveld analysis, and 1H-NMR measurements, the following conclusions can be obtained:

(1) The addition of silica powder increased the hydration rate of the low-heat cement paste, which was more obvious for the early samples. The highest improvement in hydration rate was achieved at 26% silica powder content.

(2) The increase in hydration degree mainly originates from the acceleration of the reaction rate of silica powder to C_2S, C_3A, and C_4AF, and the reaction rate of C_3S is less affected by it.

(3) As the hydration proceeded, the pore size distribution in the cement paste shifted to the gel pore region, and the macropores were reduced. silica powder reduced the calcium-silica ratio of C-S-H, further refining the paste's pore structure.

ACKNOWLEDGEMENT

This project was partially supported by a research project JSPS KAKENHI 23H00203.

The author Xia Haoran wants to show his gratitude to China Scholarship Council (CSC) for the financial support of his study in the University of Tokyo.

REFERENCES

[1] Mori, K., Fukunaga, T., Sugiyama, M., Iwase, K., Oishi, K., and Yamamuro, O., "Hydration Properties and Compressive Strength Development of Low Heat Cement," Journal of Physics and Chemistry of Solids, Vol. 73, No. 11, pp. 1274–1277, 2012.

[2] Wang, L., Yang, H. Q., Zhou, S. H., Chen, E., and Tang, S. W., "Mechanical Properties, Long-Term Hydration Heat, Shinkage Behavior and Crack Resistance of Dam Concrete Designed with Low Heat Portland (LHP) Cement and Fly Ash," Construction and Building Materials, Vol. 187, pp. 1073–1091, 2018.

[3] Chatterjee, A. K., "High Belite Cements—Present Status and Future Technological Options: Part I," Cement and Concrete Research, Vol. 26, No. 8, pp. 1213–1225, 1996.

[4] Wang, L., Dong, Y., Zhou, S. H., Chen, E., and Tang, S. W., "Energy Saving Benefit, Mechanical Performance, Volume Stabilities, Hydration Properties and Products of Low Heat Cement-Based Materials," Energy and Buildings, Vol. 170, pp. 157–169, 2018.

[5] Xie, J., Wu, Z., Zhang, X., Hu, X., and Shi, C., "Trends and Developments in Low-Heat Portland Cement and Concrete: A Review," Construction and Building Materials, Vol. 392, p. 131535, 2023.

[6] Kacimi, L., Simon-Masseron, A., Salem, S., Ghomari, A., and Derriche, Z., "Synthesis of Belite

Cement Clinker of High Hydraulic Reactivity," Cement and Concrete Research, Vol. 39, No. 7, pp. 559–565, 2009.
[7] Staněk, T., and Sulovský, P., "Active Low-Energy Belite Cement," Cement and Concrete Research, Vol. 68, pp. 203–210, 2015.
[8] Richardson, I. G., "The Nature of C-S-H in Hardened Cements," Cement and Concrete Research, Vol. 29, No. 8, pp. 1131–1147, 1999.
[9] Cau Dit Coumes, C., Courtois, S., Nectoux, D., Leclercq, S., and Bourbon, X., "Formulating a Low-Alkalinity, High-Resistance and Low-Heat Concrete for Radioactive Waste Repositories," Cement and Concrete Research, Vol. 36, No. 12, pp. 2152–2163, 2006.
[10] Segawa, M., Aili, A., and Maruyama, I., "Comparison of Shrinkage and Mass Change of Hardened Cement Paste under Gradual Drying and Rapid Drying," CEMENT, Vol. 10, p. 100047, 2022.
[11] Maruyama, I., Sakamoto, N., Matsui, K., and Igarashi, G., "Microstructural Changes in White Portland Cement Paste under the First Drying Process Evaluated by WAXS, SAXS, and USAXS," Cement and Concrete Research, Vol. 91, pp. 24–32, 2017.
[12] Ren, Y., Maruyama, I., Tomoyose, A., and Umeki, S., "Fundamental Research on Estimation of Compressive Strength of Hardened Cement Paste Mixed with Volcanic Glass Powder." Proceedings of the Japan Concrete Institute, Vol.43, No.1,2021.
[13] Maruyama, I., Fujimaki, T., Kurihara, R., Igarashi, G., and Ohkubo, T., "Surface Area Changes in C3S Paste during the First Drying Analyzed by 1H NMR Relaxometry," Cement and Concrete Research, Vol. 156, p. 106762, 2022.
[14] Muller, A. C. A., Scrivener, K. L., Gajewicz, A. M., and McDonald, P. J., "Densification of C–S–H Measured by 1H NMR Relaxometry," The Journal of Physical Chemistry C, Vol. 117, No. 1, pp. 403–412, 2013.
[15] Butler, J. P., Reeds, J. A., and Dawson, S. V., "Estimating Solutions of First Kind Integral Equations with Nonnegative Constraints and Optimal Smoothing," SIAM Journal on Numerical Analysis, Vol. 18, No. 3, pp. 381–397, 1981.
[16] Maruyama, I., Ohkubo, T., Haji, T., and Kurihara, R., "Dynamic Microstructural Evolution of Hardened Cement Paste during First Drying Monitored by 1H NMR Relaxometry," Cement and Concrete Research, Vol. 122, pp. 107–117, 2019.
[17] Scarlett, N. V. Y. and Madsen, I. C., "Quantification of phases with partial or no known crystal structures", Powder Diffraction, 21 (4): 278–284 ,2006.
[18] Mejdi, M., Wilson, W., Saillio, M., Chaussadent, T., Divet, L., and Tagnit-Hamou, A., "Quantifying glass powder reaction in blended-cement pastes with the Rietveld-PONKCS method", Cement And Concrete Research, 130: 105999 ,2020.
[19] Muller, A. C. A., Scrivener, K. L., Gajewicz, A. M., and McDonald, P. J., "Use of Bench-Top NMR to Measure the Density, Composition and Desorption Isotherm of C–S–H in Cement Paste," Microporous and Mesoporous Materials, Vol. 178, pp. 99–103, 2013.
[20] McDonald, P. J., Rodin, V., and Valori, A., "Characterisation of Intra- and Inter-C–S–H Gel Pore Water in White Cement Based on an Analysis of NMR Signal Amplitudes as a Function of Water Content," Cement and Concrete Research, Vol. 40, No. 12, pp. 1656–1663, 2010.
[21] Kurihara, R., and Maruyama, I., "Surface Area Development of Portland Cement Paste during Hydration: Direct Comparison with 1H NMR Relaxometry and Water Vapor/Nitrogen Sorption," Cement and Concrete Research, Vol. 157, p. 106805, 2022.
[22] Muller, A. C. A., Scrivener, K. L., Skibsted, J., Gajewicz, A. M., and McDonald, P. J., "Influence of Silica Fume on the Microstructure of Cement Pastes: New Insights from 1H NMR Relaxometry," Cement and Concrete Research, Vol. 74, pp. 116–125, 2015.
[23] Liao, Y., Wang, S., Wang, K., Qunaynah, S. A., Wan, S., Yuan, Z., Xu, P., and Tang, S., "A Study on the Hydration of Calcium Aluminate Cement Pastes Containing Silica Fume Using Non-Contact Electrical Resistivity Measurement," Journal of Materials Research and Technology, Vol. 24, 2023, pp. 8135–8149.
[24] Xi, J., Liu, J., Yang, K., Zhang, S., Han, F., Sha, J., and Zheng, X., "Role of Silica Fume on Hydration and Strength Development of Ultra-High Performance Concrete," Construction and Building Materials, Vol. 338, p. 127600, 2022.
[25] Siddique, R., "Utilization of Silica Fume in Concrete: Review of Hardened Properties," Resources, Conservation and Recycling, Vol. 55, No. 11, pp. 923–932, 2011.
[26] Cwirzen, A., and Penttala, V., "Aggregate–Cement Paste Transition Zone Properties Affecting the Salt–Frost Damage of High-Performance Concretes," Cement and Concrete Research, Vol. 35, No. 4, pp. 671–679, 2005.
[27] Goyal, R., Verma, V. K., and Singh, N. B., "Hydration of Portland Slag Cement in the Presence of Nano Silica," Construction and Building Materials, Vol. 394, p. 132173, 2023.
[28] Lavergne, F., Belhadi, R., Carriat, J., and Ben Fraj, A., "Effect of Nano-Silica Particles on the Hydration, the Rheology and the Strength Development of a Blended Cement Paste," Cement and Concrete Composites, Vol. 95, pp. 42–55, 2019.
[29] Bai, S., Guan, X., Li, H., and Ou, J., "Effect of the Specific Surface Area of Nano-Silica Particle on the Properties of Cement Paste," Powder Technology, Vol. 392, pp. 680–689, 2021.
[30] Gutteridge, W. A., and Dalziel, J. A., "Filler cement: the effect of the secondary component on the hydration of portland cement Part I. A Fine Non-Hydraulic Filler," Cement And Concrete Research, 20, p. 778–782,1990.